Laser Physics

PAPER

Third-order optical nonlinearities in bulk and fs-laser inscribed waveguides in strengthened alkali aluminosilcate glass

To cite this article: Gustavo F B Almeida *et al* 2018 *Laser Phys.* **28** 015401

IOP Publishing | Astro Ltd Laser Physics

Laser Phys. **28** (2018) 015401 (5pp) https://doi.org/10.1088/1555-6611/aa8ac2

Third-order optical nonlinearities in bulk and fs-laser inscribed waveguides in strengthened alkali aluminosilcate glass

Gustavo F B Almeida[1], **Juliana M P Almeida**[1], **Renato J Martins**[1], **Leonardo De Boni**[1], **Craig B Arnold**[2] and **Cleber R Mendonca**[1]

[1] Instituto de Física de São Carlos, Universidade de São Paulo, Av. Trabalhador Sãocarlense, no 400—Centro, CP369, 13.566-590, São Carlos, SP, Brazil

[2] Department of Mechanical and Aerospace Engineering, Princeton University, Princeton, NJ 08544, United States of America

E-mail: crmendon@if.sc.usp.br

Received 25 July 2017, revised 25 August 2017
Accepted for publication 25 August 2017
Published 19 December 2017

Abstract

The development of advanced photonics devices requires materials with large optical nonlinearities, fast response times and high optical transparency, while at the same time allowing for the micro/nano-processing needed for integrated photonics. In this context, glasses have been receiving considerable attention given their relevant optical properties which can be specifically tailored by compositional control. Corning Gorilla® Glass (strengthened alkali aluminosilicate glass) is well-known for its use as a protective screen in mobile devices, and has attracted interest as a potential candidate for optical devices. Therefore, it is crucial not only to expand the knowledge on the fabrication of waveguides in Gorilla Glass under different regimes, but also to determine its nonlinear optical response, both using fs-laser pulses. Thus, this paper reports, for the first time, characterization of the third-order optical nonlinearities of Gorilla Glass, as well as linear and nonlinear characterization of waveguide written with femtosecond pulses under the low repetition rate regime (1 kHz).

Keywords: femtosecond pulses, optical nonlinearities, inscribed waveguide, Gorilla Glass

(Some figures may appear in colour only in the online journal)

1. Introduction

The choice of a proper material has shown to have a crucial role in the performance of optical devices. For example, glassy materials have been pointed out as promising candidates for photonics because of their linear and nonlinear optical properties, which can be controlled by changing the chemical composition. Additionally, glasses can be processed by direct laser writing to form robust platforms for optical devices [1–3], enabling the design of three-dimensional structures within the volume of the material, opening a number of new possibilities in photonics [4–6]. Typical optical structures fabricated by femtosecond-laser micromachining include splitters and couplers [7, 8], waveplates [9], interferometers [10], ring resonators [11]. Therefore, waveguides [12–16] have been receiving a great deal of attention given their crucial role in integrated photonics devices. Special glasses, among which strengthened alkali aluminosilicates, such as Corning Gorilla® Glass—used as protective screen in mobile phones owing to its excellent mechanical and optical properties—have been shown to be suitable materials for fs-laser writing of waveguides [12, 14–16]. In this direction, investigations on the nonlinear optical properties of both bulk material and inscribed waveguides in Gorilla Glass are relevant for the proper evaluation of using such materials in the development of integrated optoelectronic and photonic devices; Gorilla Glass performance against intense laser pulses are unknown. Thus, this paper focuses on the determination of the magnitude and dynamics of third-order optical nonlinearities of Gorilla Glass, as well as on the evaluation of the linear and nonlinear performance of waveguides inscribed by fs-laser pulses in the low repetition rate regime.

2. Experimental

Third-order optical nonlinearities of Gorilla Glass, specifically the nonlinear absorption coefficient (β) and the nonlinear refractive index (n_2) were measured by the Z-scan technique [17, 18]. Response time measurements were carried out using the optical Kerr gate (OKG) technique [19]. Such experiments were performed using 150 fs pulses, at a 1 kHz repetition rate from a Ti:Al_2O_3 laser amplifier, centered at 775 nm, as the excitation source for an optical parametric amplifier (OPA) that delivers 120 fs with tunable central wavelength. Z-scan measurements were performed in the spectral range of 490–1500 nm, with pulse energy from 100 to 300 nJ and beam waist varying from 14 to 27 μm. The signal was measured by a silicon or a germanium photodetector, depending on the wavelength range. OKG measurements were carried out at 520, 650 and 790 nm. Such experiments were performed in a 700 μm thick sample. A complete description of Z-scan and OKG setups used here can be found in [20].

Femtosecond laser waveguide inscription was performed using a Ti:Al_2O_3 laser amplifier (150 fs, 1 kHz 775 nm). The pulses were focused by a microscope objective with numerical aperture (NA) of 0.65 approximately 100 μm beneath the sample surface, which was mounted on a computer controlled 3D translation stage. While inscribed waveguides longitudinal and transversal profiles were evaluated via optical microscopy, their guided modes and transmission losses were characterized in a coupling system based on objective lens setup. In this setup, the laser beam is coupled into the waveguide by an input objective (NA = 0.25) and the transmitted light is collected by an output objective (NA = 0.65). The intensity profile of the guided modes within the waveguides were analyzed by projecting its image on a CCD camera, whereas guiding losses were determined by measuring the transmitted light using a photodetector. Coupling losses were estimated by calculating the mode mismatch and taking into account objective transmission and Fresnel losses. Such characterization was performed using continuous wave (cw) at 632.8 nm and 775 nm, from a He–Ne and Ti:Al_2O_3 laser respectively.

3. Results

Closed-aperture Z-scan measurements on Gorilla Glass were performed from the visible to the telecommunications range, as shown in figure 1. As can be seen, the determined n_2 value is approximately constant in the studied spectral region (490–1500 nm), with a mean value of $3.3 \pm 0.6 \times 10^{-20}$ m^2 W^{-1}. Such results show that Gorilla Glass exhibits a nonlinear index of refraction higher than fused silica, a material commonly used for comparison purposes, whose n_2 is on the order of $2.5 \pm 0.2 \times 10^{-20}$ m^2 W^{-1} at around 1 μm [21]. Specifically at 1 μm, we obtained for Gorilla Glass an n_2 value of $3.4 \pm 0.6 \times 10^{-20}$ m^2 W^{-1}. Such a result is in agreement with the nonlinear refractive index obtained for alkaline glasses reported in the literature, whose values range from 2.2 to 3.4×10^{-20} m^2 W^{-1} [22, 23]. As is known, Gorilla Glass is strengthened via ion exchange, which results in the formation of a compression layer that extends about 150 μm below the surface. Therefore, since Z-scan measurements (figure 1) were carried out in the thin-sample regime, the measured nonlinear refractive indexes are, in fact, effective values that take into account the two compressed layers (in both sides of the sample) and the untreated layer (in the center), that comprise our sample (total length of 700 μm). In such a case, the total induced nonlinear phase is given by the sum of the nonlinear phases for each layer. Although the ion exchange process alters the glass composition and the mechanical properties of the compression layers, our results indicate that the nonlinear optical properties are not significantly affected, once the effective n_2 measured is very similar to the ones reported for the same class of glass [22, 23], i.e. the nonlinear response of the compression (strengthened) layer is equal to that of the untreated region, within the experimental error. If that was not the case, an appreciable difference (outside the experimental error) on the measured effective nonlinear refractive index would be observed. It is also interesting to point out that a nonlinear absorption signal was not observed in open-aperture Z-scan measurements over the spectral region and intensity levels (~100 GW cm^{-2}) used in the experiments.

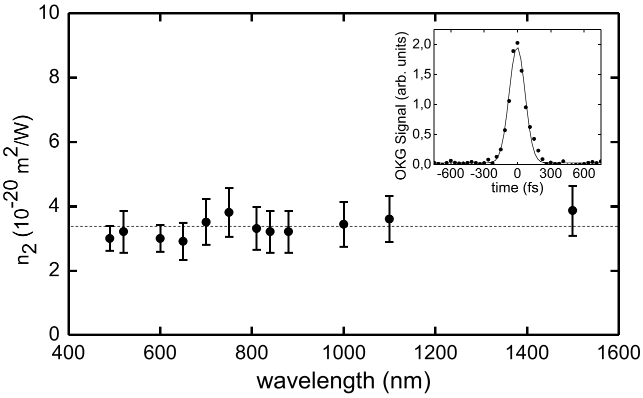

Figure 1. Nonlinear refractive index of Gorilla Glass (black) obtained by Z-scan. The dashed line is a guide for the eye. The inset displays the OKG signal at 650 nm.

The response time of the nonlinear optical effect was determined by the OKG technique, which was performed at 520, 650 and 790 nm. A typical OKG signal obtained at 650 nm is shown in the inset of figure 1. When the signal is symmetrical with respect to the zero delay time, this indicates that the observed effect is faster than the laser pulse duration. For all three wavelengths used, the response time was verified to be the same, within the experimental error. In this case, the nonlinear optical process can be considered an ultrafast electronic process.

To evaluate the potential of Gorilla Glass for photonic devices, given its optical nonlinearities, 15 mm long waveguides were inscribed 100 μm beneath the sample surface and within the compression layer by using a Ti:Al_2O_3 laser amplifier (~150 fs, 775 nm) operating at 1 kHz. Supplementary studies on the fs-laser micromachining of Gorilla Glass in the low repetition rate regime were performed (different scan speeds

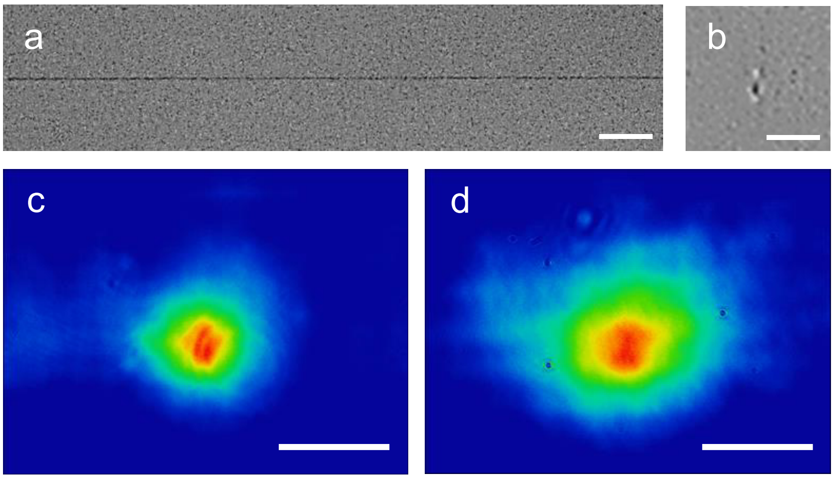

Figure 2. Microscope images of (a) longitudinal and (b) transversal profiles of waveguides fabricated at 250 nJ. Guided mode distribution at (c) 632.8 and (d) 775 nm. Scale bar in each image corresponds to 10 µm.

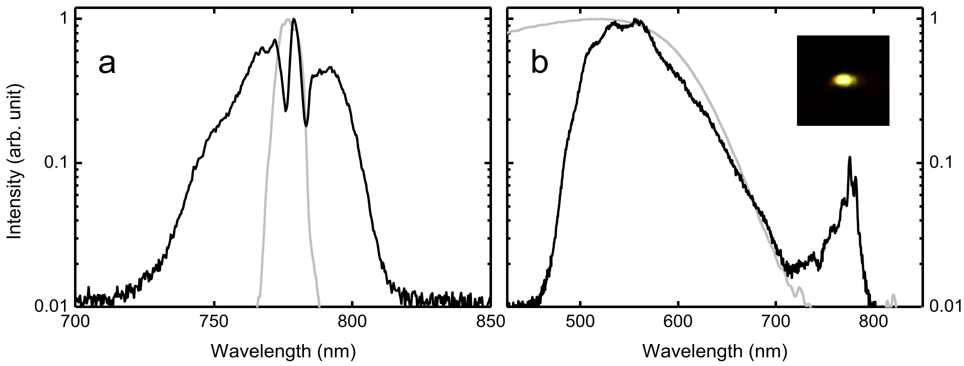

Figure 3. (a) 260 nJ input pulse spectrum (gray) and its corresponding spectral broadening after propagation in a 15 mm long waveguide. (b) Spectrum of the white-light (black) generated by a 380 nJ input pulse. The gray line displays the transmission of a filter used to block the fundamental pulse spectrum. The inset represents an image of the output guided mode.

and pulse energies), from which we determined that the sample damage occurs for a pulse energy of approximately 475 nJ (results not shown). Also, from such supplementary studies we selected the pulse energy of 250 nJ (NA $= 0.65$) and scan speed of 200 μm s^{-1} as the optimal conditions to write homogenous waveguides in Gorilla Glass, as shown by the optical microcopy images in figure 2, which displays the longitudinal section of the waveguide (a) and its symmetric transversal profile (b). The intensity distributions shown in figures 2(c) and (d) represent the guided modes obtained at (c) 632.8 nm and (d) 775 nm, both exhibiting single mode guiding, probably due to the small waveguide diameter and smooth refractive index change induced during the fs-laser inscription. By fitting the guided intensity distribution with the well known analytical solution for a step-index profile single-mode cylindrical waveguide, we were able to estimate the refractive index change to be in the order of 1×10^{-3}. Transmission measurements and calculated mismatch coefficients revealed guiding losses at both wavelengths, 632.8 and 775 nm, of 0.19 ± 0.01 dB mm^{-1} and 0.35 ± 0.01 dB mm^{-1}, respectively.

In order to study optical nonlinearities on the inscribed waveguides, 150 fs pulses at 775 nm were coupled into 15 mm long waveguides using a microscope objective with NA $= 0.25$, which is smaller than the one employed for waveguide fabrication, in such a way that the inscribed waveguides are not damaged in this experiment. Such coupling has allowed a single mode guiding, similar to the one presented in figure 2. The pulse spectra at the waveguide input and output were observed using a spectrometer added to the coupling system. For low input pulse energy (coupled energy smaller than 120 nJ), no changes in the spectral bandwidth have been observed in the output pulse spectrum (spectrum similar to the gray line shown in figure 3(a)). However, when a pulse energy of 260 nJ is coupled to the waveguide, a broadened spectrum is observed at the output, generated by the nonlinear optical effect at higher input pulses energies. The spectral broadening at the output is visualized in figure 3(a) (black) and can be compared to the input spectrum (gray). Such spectral broadening is assigned to self-phase modulation, as evidenced by the presence of the characteristic self-phase modulation peaks observed in figure 3(a) [24]. Figure 3(b) shows the wider spectral broadening (black) achieved with input pulses of 380 nJ, which is compatible with the n_2 value determined by the Z-scan measurements. The gray line in this figure displays the transmittance of the filter used to block part of the intense 775 nm laser employed. Such a white-light continuum (WLC) generated (450–800 nm) is again attributed to self-phase modulation and higher order nonlinear phase-matched processes [25]. An image of the guided mode is displayed as an inset in figure 3(b), showing that the WLC intensity distribution is rather homogeneous. As expected, the waveguide performance is not altered by the WLC generation experiment, under the conditions employed here.

Previous studies have reported spectral broadening and WLC generation resulting from ultrashort pulse propagation in tapered fibers [26]. Such studies have shown a trade-off between dispersion and nonlinearities during pulse propagation. The length scale for dispersion effects to become relevant during pulse propagation, called the dispersion length, is defined as $L_D = -T_0^2 2\pi c/(\lambda^2 D)$, in which T_0 is the pulse duration (150 fs), λ is the wavelength (775 nm), c is the speed of light, and D is the dispersion coefficient. Given that the refractive index change induced in fs-laser inscribed waveguides is on the order of 10^{-3}, its guiding properties can be interpreted in the weakly guiding regime [27], which leads to $D = -100$ fs $(\text{nm}\cdot\text{m})^{-1}$ for the waveguides fabricated here. In this way, the fs-inscribed waveguides yield $L_D \approx 1$ m and operate on the normal dispersion regime ($D < 0$). Similarly, the length scale regarding nonlinear optical effects, called nonlinear length, is defined as $L_{NL} = T_0/(\gamma E_0)$. The nonlinear optical parameter $\gamma = 2\pi n_2/(\lambda A_{eff})$ depends on the nonlinear refractive index n_2, measured by the Z-scan technique (figure 1) and on the effective area, A_{eff}, of the modal distribution, obtained from the results presented in figure 3. Estimating the coupled energy inside the waveguide as $E_0 \approx 200$ nJ, by evaluating the coupling losses, and using the laser parameter, such as pulse duration and wavelength (150 fs and 775 nm), the nonlinear length $L_{NL} \approx 2$ mm is obtained. Since the calculated dispersion length ($L_D \approx 1$ m) is much longer than the waveguide interaction length (15 mm), dispersion effects are not significant during pulse propagation. On the other hand, nonlinear optical effects, here manifested through spectral broadening and white-light generation, are expected to be observed in the case of a nonlinear length smaller than the waveguide length.

4. Conclusion

The optical nonlinearities, magnitude and time response, of bulk Gorilla Glass and the performance of fs-laser inscribed waveguides have been evaluated in the femtosecond pulse regime. Z-scan measurements revealed that the effective nonlinear index of refraction measured has a constant value on the order of $3.3 \pm 0.6 \times 10^{-20}$ m^2 W^{-1} for wavelengths ranging from 470 nm up to 1500 nm (VIS–NIR region). Such nonlinearity is responsible for generating both white-light and spectral broadening in waveguides written using femtosecond pulses of 250 nJ. The analysis of guiding modes, dispersion and nonlinear optical effect in such waveguides revealed that Gorilla Glass presents a performance comparable with other glasses, being useful for the development of integrated nonlinear optical platforms.

Acknowledgments

The authors gratefully acknowledge financial support from CNPq, CAPES, FAPESP (2011/12399-0, 2015/17058-7) and the PU-USP partnership program.

References

[1] Kruger J and Kautek W 1999 The femtosecond pulse laser: a new tool for micromachining *Laser Phys.* **9** 30–40
[2] Chichkov B N *et al* 1996 Femtosecond, picosecond and nanosecond laser ablation of solids *Appl. Phys.* A **63** 109–15
[3] Haight R *et al* 2004 High resolution material ablation and deposition with femtosecond lasers and applications to photomask repair *J. Mod. Opt.* **51** 2781–96
[4] Glezer E N *et al* 1996 Three-dimensional optical storage inside transparent materials *Opt. Lett.* **21** 2023–5
[5] Maselli V *et al* 2006 Fabrication of long microchannels with circular cross section using astigmatically shaped femtosecond laser pulses and chemical etching *Appl. Phys. Lett.* **88** 191107
[6] Deubel M *et al* 2004 Direct laser writing of three-dimensional photonic-crystal templates for telecommunications *Nat. Mater.* **3** 444–7
[7] Nolte S *et al* 2003 Femtosecond waveguide writing: a new avenue to three-dimensional integrated optics *Appl. Phys.* A **77** 109–11
[8] Eaton S M *et al* 2006 Telecom-band directional coupler written with femtosecond fiber laser *IEEE Photon. Technol. Lett.* **18** 2174–6
[9] Corrielli G *et al* 2014 Rotated waveplates in integrated waveguide optics *Nat. Commun.* **5** 4249
[10] Crespi A *et al* 2010 Three-dimensional Mach–Zehnder interferometer in a microfluidic chip for spatially-resolved label-free detection *Lab Chip* **10** 1167–73
[11] Kowalevicz A M *et al* 2005 Three-dimensional photonic devices fabricated in glass by use of a femtosecond laser oscillator *Opt. Lett.* **30** 1060–2
[12] Davis K M *et al* 1996 Writing waveguides in glass with a femtosecond laser *Opt. Lett.* **21** 1729–31
[13] Nejadmalayeri A H *et al* 2005 Inscription of optical waveguides in crystalline silicon by mid-infrared femtosecond laser pulses *Opt. Lett.* **30** 964–6
[14] Lapointe J *et al* 2014 Making smart phones smarter with photonics *Opt. Express* **22** 15473–83
[15] Lapointe J *et al* 2015 Toward the integration of optical sensors in smartphone screens using femtosecond laser writing *Opt. Lett.* **40** 5654–7
[16] Lapointe J and Kashyap R 2017 A simple technique to overcome self-focusing, filamentation, supercontinuum generation, aberrations, depth dependence and waveguide interface roughness using fs laser processing *Sci. Rep.* **7** 499
[17] Sheik-bahae M, Said A A and Van Stryland E W 1989 High-sensitivity, single-beam n_2 measurements *Opt. Lett.* **14** 955–7
[18] Sheik-Bahae M *et al* 1990 Sensitive measurement of optical nonlinearities using a single beam *IEEE J. Quantum Electron.* **26** 760–9
[19] Duguay M A and Hansen J W 1969 An ultrafast light gate *Appl. Phys. Lett.* **15** 192–4
[20] Almeida J M P *et al* 2014 Ultrafast third-order optical nonlinearities of heavy metal oxide glasses containing gold nanoparticles *Opt. Mater.* **36** 829–32

[21] Agrawal G 2013Highly nonlinear fibers *Nonlinear Fiber Optics* 5th edn (Boston, MA: Academic) pp 457–96, ch 11
[22] Grehn M *et al* 2013 Nonlinear absorption and refraction of binary and ternary alkaline and alkaline earth silicate glasses *Opt. Mater. Express* **3** 2132–40
[23] Grossmann D *et al* 2016 Transverse pump-probe microscopy of moving breakdown, filamentation and self-organized absorption in alkali aluminosilicate glass using ultrashort pulse laser *Opt. Express* **24** 23221–31
[24] Dumais P *et al* 1993 Enhanced self-phase modulation in tapered fibers *Opt. Lett.* **18** 1996–8
[25] Dudley J M *et al* 2002 Supercontinuum generation in air-silica microstructured fibers with nanosecond and femtosecond pulse pumping *J. Opt. Soc. Am.* B **19** 765–71
[26] Gattass R R *et al* 2006 Supercontinuum generation in submicrometer diameter silica fibers *Opt. Express* **14** 9408–14
[27] Gloge D 1971 Weakly guiding fibers *Appl. Opt.* **10** 2252